

Ultrafast plasma mirrors in the microwave range

C. BRAGGIO(*)

*Dipartimento di Fisica e Astronomia, Università di Padova, Padova, Italy
INFN, Sezione di Padova - Padova, Italy*

received 23 February 2015

Summary. — An experimental and numerical study of a laser-driven semiconductor mirror is detailed, which addresses two questions: whether a laser-induced semiconductor mirror is as good as a metal mirror in the microwave range and if so, at which value of photoconductivity such a metallic behavior sets in. A novel time-frequency analysis is used to investigate the properties of the mirror, based on measurements of average power transmitted through a microwave resonator. We demonstrate that a good macroscopic reflector can be realized through a semiconductor plasma, whose conductivity is orders of magnitude smaller than the one of a good metal. This non-trivial result is relevant for applications in which the mirror is requested to be switched on and off at a frequency of several gigahertz.

PACS 78.20.-e – Optical properties of bulk materials and thin films.

PACS 72.40.+w – Photoconduction and photovoltaic effects.

PACS 84.40.-x – Radiowave and microwave (including millimeter wave) technology.

PACS 06.60.-c – Laboratory procedures.

1. – Introduction

The photo-excitation of a semiconductor with short laser pulses leads to a rapid change of its optical properties in terms of reflectivity and transmittivity of incident radiation in some specified spectral ranges. Under proper experimental conditions, a laser pulse can generate in the semiconductor a dense plasma that itself acts as a mirror. This process has been extensively investigated in the past to switch $10\ \mu\text{m}$ CO_2 -laser radiation by reflection from optically induced carriers in polycrystalline germanium [1, 2], or to reflect FIR radiation by irradiating silicon with UV-laser pulses [3, 4]. More recently the idea to achieve reflection by materials whose optical properties are modified through laser pulses has been exploited to realize active mirrors for ultrahigh-intensity optics [5]. A renewed interest in the development of ultrafast laser-induced mirrors has

(*) caterina.braggio@unipd.it

been formulated in a recent proposal to detect a quantum electrodynamics (QED) effect, namely the optomechanical coupling between an ensemble of Rydberg atoms and an oscillating wall [6]. In this peculiar application, the mirror is requested to be turned on and off at a frequency of several GHz to match the dipole transitions of the Rydberg atoms. Besides possible applications to the development of ultrafast all-optical switches and parametric amplification processes in the microwave regime, the potential of such mirror has long been recognized also to change non-adiabatically the boundary conditions of the vacuum state of the electromagnetic field [7], a phenomenon of particular interest in a three-dimensional microwave resonator [8].

The presented mirror approach is based on the possibility to control a fast semiconductor conductivity by multi-GHz repetition rate laser pulses, as those delivered by mode-locked sources [9]. The oscillation frequency of the switching mirror would then coincide with the laser pulses repetition rate, as long as the recovery time of the semiconductor is smaller than the period between the laser pulses. In principle, 100 GHz switching frequency could be achieved with an effective mirror based on a semiconductor whose recovery time is of a few ps. Short recombination times can be found, for example, in low-temperature-grown GaAs or by damaging the crystalline structure of a semiconductor through ion irradiation [10-14]. In addition, mode-locked oscillators with repetition rates as high as 10 GHz and 200 pJ pulse energy have been demonstrated [15]. It is then crucial to understand if such a laser pulse energy is sufficient to generate a good macroscopic (several square mm area) mirror. This issue is investigated in sects. 3 and 4, whereas sect. 2 is devoted to the description of the preparation and characterization of the ultrafast bulk semiconductor samples.

2. – A short-recombination-time semiconductor

As previously mentioned, short-carrier-lifetime semiconductors can be produced through ion irradiation. In particular, light-ion irradiation of GaAs substrates generates isolated point defects, corresponding to mid-gap states which act as fast recombination centers of the photoexcited carriers [13, 14]. Low-temperature-grown gallium arsenide [10, 16] also exhibits short recombination times, yet it is not considered here because of its Hall mobility that is found to be low [17]. In contrast, SI-GaAs has a very high value of mobility ($\geq 6000 \text{ cm}^2/\text{Vs}$), which is preserved after the light-ion irradiation procedure, as long as the dose is maintained at reasonable values [14]. Figure 1 shows the differential terahertz transmission amplitude through SI-GaAs disks that have been subjected to a 5.2 MeV proton dose ranging from 1.2 to 12 in units of 10^{14} protons/cm². A THz-TDS (terahertz time-domain spectroscopy) apparatus based on photoconductive antennas [18], activated by ~ 50 fs-duration, 790 nm-wavelength laser pulses from a Ti:Sa oscillator (model TiF-50, Avesta Project), is used to characterize the proton-irradiated samples. In the inset of fig. 1 the spectrum of the THz radiation that probes the GaAs samples is shown. The first requirement to realize a dynamic mirror is satisfied by the highest-irradiation-dose samples, whose exponential decay signal has a characteristic time of about 5 ps.

3. – The bulk semiconductor plasma properties

We investigate the properties of the semiconductor plasma inside a microwave resonator, with the experimental setup shown in fig. 2. A semiconductor disk is placed over one of the walls of a microwave cavity whose parameters, namely the frequency of

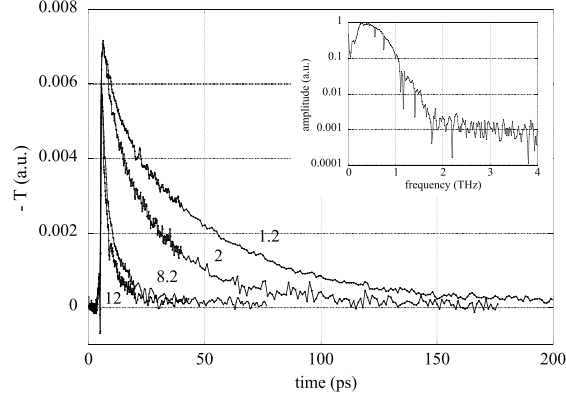


Fig. 1. – Results of the optical pump-THz probe measurement on different-irradiation-dose samples. The number next to each curve indicates the dose in units of 10^{14} protons/cm². The pump pulse energy is $E = 4.4$ nJ. The inset shows the probe spectrum.

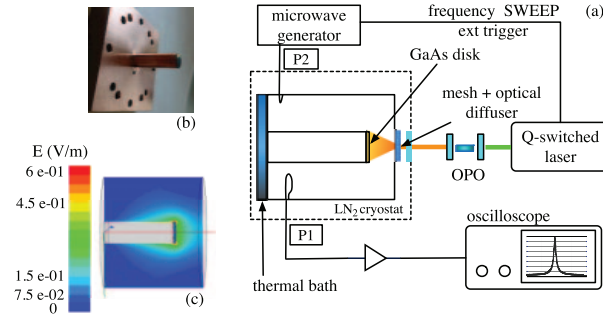


Fig. 2. – (a) Schematic of the experimental setup to measure the microwave resonator parameters in the presence of a transient plasma in the GaAs disk. Lorentz resonance curves are registered at an oscilloscope when several values of the generator frequency are swept through the cavity in P2 and their corresponding transmission level at P1 is amplified and measured at a fixed delay after the Q -switched laser pulse excitation. (b) Picture of the re-entrant cylinder with the GaAs disk glued to its top and (c) plot of the electric field in the cavity resonator as obtained by numerical simulations.

resonance f_0 and the loaded quality factor Q_L , are measured for different values of the incident laser pulse energy E_p (*i.e.* different plasma concentrations).

As the photo-induced concentration changes in time, it is not possible to apply the traditional transmission spectroscopy methods to obtain the cavity parameters in the presence of the semiconductor plasma. In fact, with spectrum and vector analyzers, or even the cavity field decay time method, only resonators in stationary conditions can be characterized. Therefore we devise a new method, whereby the power transmitted through the cavity is measured at different frequencies in the time domain, at a fixed time following the laser excitation. The re-entrant cylinder cavity geometry is chosen, because a maximum cavity perturbation can be realized when the semiconducting crystal covers

the top of the internal cylinder. The electric field is in fact concentrated in the gap, as shown by the plot of the electric field magnitude obtained by means of the finite-element analysis (fig. 2(c)). The internal and external cylinder diameters are 8.35 and 43 mm, respectively, their height 22 and 27 mm. The cavity, which has been machined out of bulk copper, is used in the lowest-frequency mode, the TM_{010} mode. A good thermal contact is ensured between the cavity and the bottom of a liquid-nitrogen temperature vessel, and the sensor S measured a temperature of 78 K during the present measurements. A $\langle 100 \rangle$ -oriented SI-GaAs disk (thickness $160 \mu\text{m}$, 8.35 mm diameter) is used to investigate the properties of the plasma mirror.

To achieve generation at $\lambda = 806 \text{ nm}$ we pump an Optical Parametric Oscillator (OPO) cavity with 532 nm-wavelength, 10 ps-duration pulses delivered by a Q -switched laser source (model GIANT, Quanta System) to achieve generation at $\lambda = 806 \text{ nm}$. This wavelength corresponds to a photon energy of 1.54 eV, sufficient to excite the electron-hole pairs to the bottom of the conduction band of GaAs [19]. Light impinges on the semiconductor through an aperture, whose diameter is comparable with the internal cylinder of the cavity. The aperture is covered by a copper mesh composed of $100 \mu\text{m}$ wires, with a spatial period of 0.5 mm, supported by a 1 mm-thickness sapphire disk. Uniform illumination of the semiconductor disk surface is achieved by means of an optical diffuser (angular aperture = 0.6), set before the cavity aperture.

At liquid-nitrogen temperature the measured cavity parameters hosting the unperturbed GaAs disk are $f_0 = 2.3292 \text{ GHz}$ and $Q_0 = 5930$. The cavity has two ports P1 and P2 for the transmission spectroscopy with coupling coefficients β_1 and β_2 , respectively. The input port P2 has a weak coupling with the cavity magnetic field ($\beta_2 \ll 1$), whereas β_1 can be adjusted to obtain critical coupling ($\beta_1 = 1$), *i.e.* the condition whereby the power absorbed in the cavity equals the power dissipated along the transmission line [20]. The frequency sweep of a microwave generator is controlled in such a way that at each laser pulse a new value of frequency is sent in port P2. The transmitted signal in P1 is then amplified by a low-noise microwave amplifier (Miteq AFD3 023027-08-S), whose gain is 33 dB. For each frequency value, an oscilloscope registers the root-mean-square amplitude within a 10 ns gate, opened $1 \mu\text{s}$ after the laser excitation. Some representative transmission curves that are obtained for different values of the incident laser pulse energy E_p are shown in fig. 3. E_p is changed from a maximum of approximately 5 mJ to $10 \mu\text{J}$, in which the lowest values of energy are achieved by means of calibrated absorptive filters. The initial photo-conductivity σ_0 is related to E_p as

$$(1) \quad \sigma_0 = e n_0 (\mu_e + \mu_h) \approx e n_0 \mu_e = \left[\frac{E_p}{h\nu} (1 - R) \eta \frac{\alpha}{S} \right] e \mu_e,$$

where n_0 is the photo-induced initial concentration, $h\nu \sim 1.54 \text{ eV}$ is the incident photon energy, $R = 0.3$ and $\eta = 0.9$ are respectively the semiconductor reflectivity and quantum efficiency. The electron mobility of semi-insulating GaAs at 77 K is $\mu_e = 20 \cdot 10^4 \text{ cm}^2/\text{Vs}$ [19, 21], much higher than the hole mobility μ_h that has thus been dropped. S is the illuminated semiconductor surface and the absorption coefficient α at the incident photon wavelength is 10^4 cm^{-1} [19]. For a numerical example, if $E_p = 10 \text{ nJ}$ the initial photo-induced conductivity is about $3.7 \cdot 10^3 \text{ Sm}^{-1}$. Each series of transmitted amplitude *vs.* frequency data is fit to a Lorentzian curve using a nonlinear least-squares fit, in which the resonant frequency f_0 , loaded quality factor Q_L , constant background A_1 , and maximum of the transmission coefficient A_2 , are used as fitting parameters [22]. The variation of the cavity parameters is shown in the inset of fig. 3 for several values

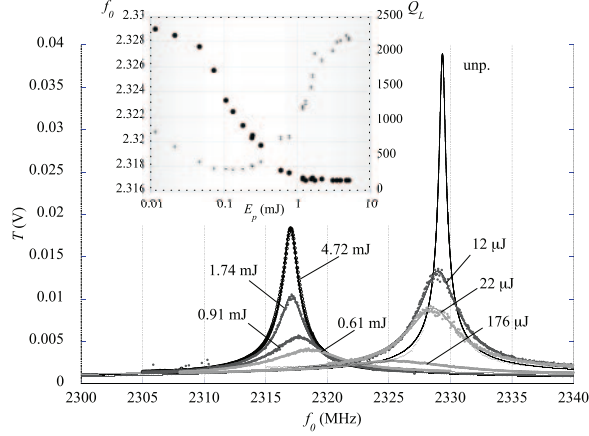


Fig. 3. – Time-domain transmission spectroscopy. Each series of data, corresponding to a different value of the incident laser pulse energy E_p , is fitted to a Lorentzian function in the form $T(f) = A_1 + A_2/\sqrt{1 + 4Q_L^2(f/f_0 - 1)^2}$ to infer the cavity parameters f_0 and Q_L displayed in the inset. The unperturbed cavity resonance (label “unp”) is also reported.

of the incident laser pulse energy. It is observed that the cavity resonance frequency decreases for increasing E_p down to a minimum value. Therefore, once a threshold photo-induced concentration is achieved, the frequency no longer decreases if the laser pulse energy is further increased. This saturated value of frequency corresponds to the frequency of the smaller gap cavity, *i.e.* a re-entrant cavity with the GaAs disk replaced by a metallic disk. The quality factor is minimum when the slope of the frequency variation is maximum, and for highest values of photo-injection the smaller gap cavity displays a Q_L value that is comparable with the unperturbed loaded quality factor ($Q_L \approx 2800$).

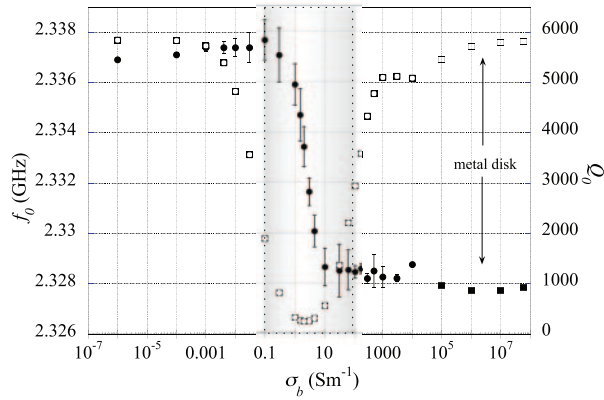


Fig. 4. – Finite-elements analysis results. The filled dots represent the frequency data whereas the empty ones refer to the unloaded quality factor Q_0 , calculated for several values of the GaAs bulk conductivity σ_b . If a metal disk replaces the semiconductor, the data indicated by the square symbols are obtained.

4. – Numerical simulations

In order to assess the experimental results shown in fig. 3, the stationary cavity parameters f_0 and Q_0 are numerically calculated by means of the finite-elements analysis. The modeled cavity has the following properties: 1) a conductivity of $5.3 \cdot 10^7 \text{ Sm}^{-1}$ is assigned to its walls so as to obtain the same value of the unperturbed quality factor experimentally measured, 2) the $160 \mu\text{m}$ -thick GaAs disk is characterized by a bulk conductivity σ_b , that simulates the action of the laser pulse. The latter assumption should not limit the simulation results because in the transmission measurements shown in fig. 3, the dynamics of the semiconductor plasma mirror is “frozen” at $t = 1 \mu\text{s}$ after the laser excitation, when, due to ambipolar diffusion processes and the recombination of the photo-excited carriers, a $\sigma_b \ll \sigma_0$ is reached in the overall semiconductor. The calculated cavity parameters are reported in fig. 4 for several values of σ_b in the range 10^{-7} – 10^4 . In the same graph the results obtained by the simulations if the semiconductor is replaced by a metal are displayed. It is evident that both the frequency and quality factor data in the range 0.1 – 100 Sm^{-1} well reproduce the behavior shown in fig. 3. Note that in the reported measurements the energy per pulse also spans three decades. The finite-elements analysis demonstrates that the perfect reflector task is accomplished by a laser-excited plasma whose conductivity is of the order of 10^3 Sm^{-1} , much smaller than a typical good metal conductivity.

We also note that the presented artificial mirror does not match the simple picture of good conductor given by the skin depth theory. When the so-called low frequency approximation [23] is satisfied, the incident field penetrates the boundary (mirror) a distance that can be quantified by the skin depth $\delta = \sqrt{2\epsilon_0 c^2 / \sigma \omega}$ and gets reflected. The thickness of the demonstrated mirror is instead much smaller than the 1 mm calculated skin depth. This result is in agreement with previous results obtained with metallic films, that exhibit good reflectivities up to very small thicknesses, much smaller than the calculated skin depth at microwave and radio frequencies [24].

In conclusion, a semiconductor plasma mirror in the microwave range has been demonstrated, that exhibits unitary reflection with a photo-induced conductivity that is several orders of magnitude smaller than the conductivity of a metal. This important result, that is supported by the experimental verification of the mirror, allows to relax the requirements regarding the mode-locked laser system to be employed in the dynamic mirror. In fact, the photo-induced concentration of carriers would then be of the order of $n = \sigma / e\mu_e = 3.1 \cdot 10^{12} \text{ cm}^{-3}$. In a few square mm area mirror, such a concentration can be induced, for example, with approximately 200 pJ energy pulse, readily available at the output of a 10 GHz repetition rate Nd:YVO₄ mode-locked laser oscillator [15], in CW pulses and without any need for further optical amplification. This work opens then the possibility to realize the dynamic mirror for the mentioned QED experiments and can be of importance for optoelectronics applications.

* * *

The author would like to thank D. IANNUZZI and A. ORTOLAN for their critical reading of the manuscript. Financial support of the University of Padova under Progetto di Ateneo 2013 (cod. CPDA135499/13) is gratefully acknowledged.

REFERENCES

- [1] ALCOCK A. J., CORKUM P. B. and JAMES D. J., *Appl. Phys. Lett.*, **27** (1975) 680.
- [2] JAMISON S. A. and NURMIKKO A. V., *Appl. Phys. Lett.*, **33** (1978) 598.
- [3] VOGEL T., DODEL G., HOLZHAUER E., SALZMANN H. and THEURER A., *Appl. Opt.*, **31** (1992) 329.
- [4] WILSON T. E., *Phys. Rev. B*, **59** (1999) 12996.
- [5] THAURY C., QUERE F., GEINDRE J.-P., LEVY A., CECCOTTI T., MONOT P., BOUGEARD M., REAU F., D'OLIVEIRA P., AUDEBERT P., MARJORIBANKS R. and MARTIN PH., *Nature*, **3** (2007) 424.
- [6] ANTEZZA M., BRAGGIO C., CARUGNO G., NOTO A., PASSANTE R., RIZZUTO L., RUOSO G. and SPAGNOLO S., *Phys. Rev. Lett.*, **113** (2014) 023601.
- [7] YABLONOVITCH E., HERITAGE J. P., ASPNES D. E. and YAFET Y., *Phys. Rev. Lett.*, **63** (1989) 976.
- [8] BRAGGIO C., BRESSI G., CARUGNO G., DEL NOCE C., GALEAZZI G., LOMBARDI A., PALMIERI A., RUOSO G. and ZANELLO D., *Europhys. Lett.*, **70** (2005) 754.
- [9] KELLER U., *Nature*, **424** (2003) 831.
- [10] KROTKUS ARŪNAS, *J. Phys. D*, **43** (2010) 273001.
- [11] JOHNSON M. B., MCGILL T. C. and PAULTER N. G., *Appl. Phys. Lett.*, **54** (1989) 2424.
- [12] STELMAKH N., MANGENEY J., ALEXANDROU A. and PORTNOI E. L., *Appl. Phys. Lett.*, **73** (1998) 3715.
- [13] MANGENEY J., STELMAKH N., ANIEL F., BOUCAUD P. and LOURTIOZ J.-M., *Appl. Phys. Lett.*, **80** (2002) 4711.
- [14] NĚMEC H., FEKETE L., KADLEC F., KUŽEL P., MARTIN M., MANGENEY J., DELAGNES J. C. and MOUNAIX P., *Phys. Rev. B*, **78** (2008) 235206.
- [15] KRAINER L., PASCHOTTA R., LECOMTE S., MOSER M., WEINGARTEN K. J. and KELLER U., *IEEE J. Quant. Electron.*, **38** (2002) 1331.
- [16] LOUKAKOS P. A., KALPOUZOS C., PERAKIS I. E., HATZOPOULOS Z., LOGAKI M. and FOTAKIS C., *Appl. Phys. Lett.*, **79** (2001) 2883.
- [17] GUPTA S., FRANKEL M. Y., VALDMANIS J. A., WHITAKER J. F., MOUROU G. A., SMITH F. W. and CALAWA A. R., *Appl. Phys. Lett.*, **59** (1991) 3276.
- [18] DEXHEIMER S. L., *Terahertz Spectroscopy: Principles and Applications* (CRC Press, Taylor and Francis Group) 2008.
- [19] BLAKEMORE J. S., *J. Appl. Phys.*, **53** (1982) R123.
- [20] PADAMSEE H., KNOBLOCH J. and HAYS T., *RF Superconductivity for Accelerators* (Wiley-VCH) 2008.
- [21] RUZICKA BRIAN A., WERAKE LALANI K., SAMASSEKOU HASSANA and ZHAO HUI, *Appl. Phys. Lett.*, **97** (2010).
- [22] PETERSAN P. J. and ANLAGE S. M., *J. Appl. Phys.*, **84** (1998) 3392.
- [23] FEYNMAN R. P., LEIGHTON R. B. and SANDS M., *The Feynman Lectures on Physics* (Addison-Wesley) 1966.
- [24] KAPLAN A. E., *Radio Eng. Electron. Phys.*, **9** (1964) 1476.